Line Sampling for Time-variant Failure Probability Estimation Using an Adaptive Combination Approach

Xiukai Yuan[a], Weiming Zheng[a], Chaofan Zhao[a], Marcos A. Valdebenito[b], Matthias G.R. Faes[b], Yiwei Dong[a,*]

[a]*School of Aerospace Engineering, Xiamen University, Xiamen 361005, P. R. China*
[b]*Chair for Reliability Engineering, TU Dortmund University, Leonhard-Euler-Strasse 5, 44227 Dortmund, Germany.*

Abstract

An efficient sampling approach 'Adaptive Combined Line Sampling' is proposed for evaluating the 'time-variant failure probability function' (TFPF) of structures. Line Sampling is implemented in an adaptive and iterative way, where each individual Line Sampling run is carried out based on adaptively selected important directions, in order to ensure a sufficiently precise estimation of the TFPF over the whole time interval of analysis. An adaptive strategy and an optimal combination algorithm are developed for the practical implementation of the Line Sampling process. The adaptive strategy allows to determine the optimal important direction which is then used in the next Line Sampling run. The combination strategy allows to collect all these adaptive sampling runs together in an optimal way, which aims at minimising the coefficient of variation (C.o.V.) of the TFPF estimate. Due to these strategies, the proposed approach can estimate the TFPF in a more efficient way than the traditional Line Sampling, while guaranteeing that the C.o.V. of the estimate remains below a prescribed threshold over the whole time of analysis. Thus it can be seen as an extended version of classical Line Sampling specially tailored for time-variant reliability analysis. Examples are given to illustrate the performance of the proposed approach.

Keywords: Time-variant reliability analysis, Line sampling, Adaptive strategy, Cumulative failure probability function, Composite limit state functions

1. Introduction

Time-variant reliability analysis considers uncertainty in the time-variant properties and loading when assessing the level of safety of a structural system, and has attracted much attention recently. This is due to the fact that engineering structures and systems usually suffer from the deterioration of structural strength and stiffness with time under severe operating or environmental conditions during their service life [1]. Following this framework, it is assumed that the system parameters and loading are characterised as stochastic process, instead of static random variables, to represent their natural variability with respect to time. In this context, a reliability analysis can properly reflect and quantify the effect of time-variant factors by estimating the failure probability of a system/structure over a period of time, which is termed as time-variant (or time-dependent) failure probability function. Compared with traditional, static reliability analysis, more challenges are faced in time-variant reliability analysis because an extra dimension (time) is involved. Due to the time-dependency of structural properties, loading as well as the structural system failure events, time-variant reliability analysis is even more computationally involved when compared with static reliability analysis. Several numerical methods have been proposed to conduct time-variant reliability analysis. These methods can be roughly classified into three groups: analytical techniques, simulation-based approaches and surrogate models. Analytical methods usually involve approximation concepts. For example, Jiang et al. [2] used the first-order reliability method (FORM) to estimate the failure probability after converting the associated stochastic processes into a set of random variables by time discretisation and linearisation of the performance function. Mourelatos et al. [3] combined FORM with the total probability theorem to evaluate the time-variant reliability after transforming the target time-variant problem into one with composite performance functions. In [4], the time-variant reliability problem is solved using classical approaches for time-invariant reliability (such as FORM) by focusing on outcrossing rates and a parallel system analysis. Zhang et al. [5] propose a moment-based PHI2 (MPHI2) method for time-variant reliability analysis of structures to reduce the computational cost by separating the finite element analysis from the analysis cycle and estimating the statistical characteristics of the associated components beforehand.

The second class of approaches for solving time-variant reliability problems involves simulation methods. In fact, simulation-based methods for static system reliability analysis can be applied in time-variant problems. In this context, namely time-invariant problems, many highly efficient simulation methods have been developed. For instance, Line Sampling (LS) [6] has been developed for estimating the reliability of static and dynamical systems. Further, De Angelis et al. [7] developed an Advanced Line Sampling method to compute interval failure probabilities when both aleatory and epistemic uncertainties are considered. Shayanfar et al. [8] introduced an adaptive line sampling method for reliability analysis by updating the importance direction during the sampling process and averaging different estimations to form a final one. Au and Beck [9] proposed an efficient Importance Sampling method for linear dynamical systems. Misraji et al. [10] applied a Directional Importance Sampling scheme to analyse the reliability of structural systems subject to stochastic dynamic Gaussian loading. Subset simulation [11] also provides an efficient and effective way to address reliability problems in high-dimensional spaces which involve a large number of random variables. Recently, Li et al. [12] proposed a Generalised Subset Simulation to handle high-dimensional, time-variant reliability problems. Chakraborty et al. [13] introduced two innovative methods based on Subset Simulation (SS) for time-dependent system reliability analysis and the space-time-variant reliability analysis, offering solutions to the challenge of assessing the reliability of corroding pipelines. Similarly, Du et al. [14] adopted Parallel Subset Simulation to handle time-variant reliability with both deterioration in material properties and dynamic load. Yuan et al. [15] proposed an efficient two-step Importance Sampling to estimate the time-variant reliability where the limit state function includes structural degradation parameter processes, random variables, and Gaussian stochastic load processes. Zhang et al. [16] proposed a single-loop approach for time-variant reliability evaluation combined with a weighted sampling strategy for moment assessment.

Surrogate models, especially Gaussian process (GP) or Kriging regression, have been widely used in reliability analysis, as well as in time-variant reliability. Xu and Saleh [17] also reviewed the use of machine learning for reliability engineering and safety applications involving time-variant problems. Li et al. [18] proposed a deep learning framework for time-dependent reliability analysis of dynamic systems, with local-limit state functions and global surrogate models, to capture the long-term dependency of system dynamics and estimate time-dependent reliability. In addition, some contributions focus on the implementation of surrogate models that cooperate with simulation-based methods with the purpose of further reducing numerical costs associated with time-variant reliability assessment. Wang and Wang [19] adopted a sequentially updated Gaussian process model to characterise extreme system response over time, and then Monte Carlo simulation is employed to assess the time-variant reliability. Depina et al. [20] used Kriging within the framework of the Line Sampling. Wu et al. [21] proposed a Parallel Efficient Global Optimization strategy integrated with adaptive Kriging-Monte Carlo simulation for time-variant problems. Zhao et al. [22] proposed a nested single-loop Kriging model coupled with Subset Simulation to evaluate time-dependent system reliability. Zhang et al. [23] proposed an active learning method based on deep neural networks and a weighted sampling method to address cases involving interval processes. However, discrete representation of stochastic processes increases the dimensions of the reliability problem, posing a challenge for surrogate modelling due to the so-called *curse of dimensionality*. In this sense, to the knowledge of the authors, there is still plenty of room for improvement regarding simulation-based methods for time-variant reliability.

In view of the aforementioned difficulty in estimating the structural time-variant reliability as a function of time, an efficient approach termed as 'Adaptive Combined Line Sampling' (ACLS) is proposed. This approach is developed by applying the composite limit state concept, which first transforms the time-variant reliability problem into an equivalent problem involving a series system. Then, Line Sampling is applied in an iterative and adaptive manner, and at the last step, an optimal combination algorithm is developed to obtain the overall time-variant failure probability function estimate. The combination is based on the principle of minimising a statistical descriptor of the estimate (e.g. variance), as proposed in [8, 24, 25]. The innovative aspects of this contribution with respect to the state-of-the-art are as follows.

- A simulation-based method which can produce satisfactory, accurate estimations of the failure probability as a function of time is developed.
- The most salient feature of the proposed approach is that it can ensure good precision for estimating the TFPF by virtue of the aforementioned adaptive strategy.
- The optimal combination algorithm enhances the precision and efficiency of the proposed approach.

The remainder of this paper is organised as follows. First, the definition and the composite limit states transformation associated with the time-dependent reliability problem are briefly reviewed in Section 2. Then, the mathematical formulation of the proposed framework is developed in Section 3. Next, Section 4 illustrates the performance of the proposed approach through three examples. Finally, the paper closes with discussions and an outlook for future work in Section 5.

2. Time-variant reliability

2.1. Definition

In this contribution, the quantity of interest is the corresponding failure probability over a given time period which is given by:

$$P_F(t) = P\left\{g(\boldsymbol{x}, \tau, \boldsymbol{y}(\tau)) \leq 0, \exists \tau \in [0, t]\right\}, \tag{1}$$

where $\boldsymbol{x} = [x_1, x_2, \dots, x_n]$ is the vector of time-invariant random variables associated with the structure/system with probability density function (PDF) $f_X(\boldsymbol{x})$; $\exists$ stands for 'there exists at least one'; $\tau \in [0, t]$ indicates that $P_F(t)$ is a cumulative failure probability which considers all the instantaneous cases from 0 up to time instant t, and $t \in [0, T]$ where T denotes the time window of analysis; $\boldsymbol{y}(t) = [y_1(t), \dots, y_{n_y}(t)]$ is the vector of time-dependent stochastic processes describing the evolution of structural properties or loads, which are implicit with respect to time t; and $g(\cdot)$ is the performance function. This is the most general type of time-variant problem, as it encompasses random variables, explicit time-dependent properties (such as structural degradation processes), and time-dependent stochastic processes (such as stochastic load processes).

2.2. Transformation of time-variant reliability problem by composite limit states

The time-variant reliability problem can be transformed into a time-invariant problem with a series of instantaneous performance functions. This is a common approach for structural time-variant reliability analysis which is called 'composite limit states' [12]. The basic idea of this approach is to use the concept of series system reliability of the instantaneous performance functions to convert the time-dependent reliability problem into a time-invariant one. Indeed, a time-variant performance function can be represented discretely as follows. First, the time interval $[0, T]$ is discretised using a time step size Δt. Then, a time sequence $[t_0, \dots, t_l \dots, t_{n_t}] = [0, \dots, l\Delta t, \dots, n_t\Delta t]$ is generated, where $l = 0, \dots, n_t$ is the time index, $t_0 = 0$ and $t_{n_t} = n_t\Delta t = T$. Based on the series system reliability formulation, the cumulative failure probability at a time instant t_l over a certain time period $[0, T]$ is given by:

$$P_F(t_l) = P\left\{\bigcup_{i=0}^{l} F_i\right\} = P\left\{\min_{i=0,\dots,l} g(\boldsymbol{x}, t_i, \boldsymbol{y}(t_i)) \leq 0\right\}, \; l = 0.\dots, n_t, \tag{2}$$

where $F_i = \{g(\boldsymbol{x}, t_i, \boldsymbol{y}(t_i)) \leq 0\}$ is the instantaneous failure region associated with the limit state function at the i-th time instant and $t_l = l\Delta t$ is the time instant at which the time-variant failure probability is being calculated.

For the stochastic processes $\boldsymbol{y}(t)$, spectral decomposition methods such as the Karhunen-Loève (K-L) expansion [26, 27] or the Expansion Optimal Linear Estimator (EOLE) [28] can be adopted to transform the random process $\boldsymbol{y}(t)$ into a function of random variables $\boldsymbol{z}$. Note that there are different kinds of random processes [29, 30]. In this work, only Gaussian processes are considered. Note that the proposed approach can be applied whenever a more general stochastic process can be represented as a nonlinear function of a Gaussian process. Then, the instantaneous performance function $g(\boldsymbol{x}, t_i, \boldsymbol{y}(t_i))$ can be rewritten as $g_z(\boldsymbol{x}, t_i, \boldsymbol{z})$ in the coordinate space $(\boldsymbol{x}, \boldsymbol{z})$, where $\boldsymbol{z}$ is the vector collecting all normal random variables associated with the representation of the random process $\boldsymbol{y}(t)$. The corresponding cumulative failure probability, as defined in Eq. (2), is expressed as:

$$P_F(t_l) = \iint I_{F_{t_l}^U}(\boldsymbol{x}, t_l, \boldsymbol{z}) f_X(\boldsymbol{x}) \phi(\boldsymbol{z}) \, \mathrm{d}\boldsymbol{x} \, \mathrm{d}\boldsymbol{z}, \tag{3}$$

where $F_{t_l}^U = \bigcup_{i=0}^{l} \{F_i : g_z(\boldsymbol{x}, t_i, \boldsymbol{z}) \leq 0\}$ is the union of failure events of the series system; $I_{F_{t_l}^U}(\cdot)$ is the indicator function associated with $F_{t_l}^U$; and $\phi(\cdot)$ is the joint PDF of i.i.d. standard normal variables. Note that the computation of this failure probability function with respect to time t is quite challenging, as it comprises an evolving series system with respect to time. In fact, most of the existing methods for reliability analysis can handle point-wise failure probability, that is, at a fixed time instant $t = T$. However, it may become troublesome to estimate the failure probability as a function of time with classical reliability methods while maintaining the accuracy and efficiency. Thus, in this work, a novel approach is proposed to solve the time-variant failure probability function in an efficient and effective way.

3. Proposed approach

3.1. Overview of the proposed approach

This section outlines the proposed Adaptive Combined Line Sampling (ACLS) approach for TFPF estimation. Although Line Sampling and Advanced Line Sampling have been proposed and widely applied in many fields, its application in time-variant reliability still needs further investigation. The reason is that, while both approaches work well for failure probability estimation in a time-invariant setting, their application to time-variant problems may be demanding, as it becomes necessary to estimate all failure probabilities associated with each time instant. In other words, classical Line Sampling is not suitable for estimating a failure probability function dependent on time. Hereto, a novel variant of Line Sampling, where an adaptive learning strategy and an optimal combination algorithm are applied, is proposed to address the challenge of estimating TFPF efficiently. In the proposed approach, the final TFPF estimator $\hat{P}_F^{(m)}(t_l)$ is constructed based on combining a number of m individual estimators, that is:

$$\hat{P}_F^{(m)}(t_l) = \sum_{k=1}^{m} w_k(t_l)\hat{P}_{F,k}(t_l), \tag{4}$$

where $\hat{P}_{F,k}(t_l)$ is the estimator evaluated by the $k-th$ run of Line Sampling; m is the number of runs performed with Line Sampling, which is determined on-the-fly as the stopping criterion is reached (please see Section 3.5); and $w_k(t_l)$ denotes a weight function. Note that $\sum_{k=1}^{m} w_k(t_l) = 1$ is imposed for each time instant $t_l = l\Delta t(l = 0, \ldots, n_t)$. Thus, as long as $\hat{P}_{F,k}(t_l)$ is unbiased [6], then the obtained $\hat{P}_F^{(m)}(t_l)$ is also unbiased. Under the assumption that each run of Line Sampling component is carried out separately, the TFPF components,that is, $\hat{P}_{F,k}(t_l)$, are mutually independent, and the variance of $\hat{P}_F^{(m)}(t_l)$ can be easily obtained as:

$$Var\left[\hat{P}_F^{(m)}(t_l)\right] = \sum_{k=1}^{m} w_k^2(t_l)Var\left[\hat{P}_{F,k}(t_l)\right], \tag{5}$$

Further, if all the TFPF components, $\hat{P}_{F,k}(t_l)$, are unbiased estimators, i.e., $E[\hat{P}_{F,k}(t_l)] = P_F(t_l)$, then the coefficient of variation (C.o.V.) of $\hat{P}_F^{(m)}(t_l)$ is given by

$$Cov[\hat{P}_F^{(m)}(t_l)] = \frac{\sqrt{\sum_{k=1}^{m} w_k(t_l)^2 Var[\hat{P}_{F,k}(t_l)]}}{P_F(t_l)} = \sqrt{\sum_{k=1}^{m} w_k^2(t_l)Cov^2[\hat{P}_{F,k}(t_l)]}, \tag{6}$$

The proposed approach consist of three steps: 1) Estimate the TFPF component by Line Sampling; 2) Find the next time instant to carry out Line Sampling by an active strategy; 3) gather the TFPF component estimates by optimal combination. Each of these steps is discussed in detail below.

3.2. Estimate the TFPF by Line Sampling

As stated in Eq.(4), the final TFPF estimator is constructed by aggregating a number of TFPF components. In this subsection, Line Sampling [6, 31] is adopted to calculate the component TFPF estimator $\hat{P}_{F,k}(t)$.

For the sake of simplicity, it is assumed that the time-invariant random variables associated with $\boldsymbol{x}$ follow a standard normal probability distribution. Such condition can be satisfied by considering appropriate transformations, see e.g., [32]. Then, to implement Line Sampling, it is necessary to identify an *important direction* $\boldsymbol{\alpha}^{(k)}$, which is a vector of unit Euclidean norm located at the origin of the standard normal space which points towards the failure region associated with the component TFPF estimator $\hat{P}_{F,k}(t)$. A criterion for selecting this important direction $\boldsymbol{\alpha}^{(k)}$ is:

$$\boldsymbol{\alpha}^{(k)} = \frac{(\boldsymbol{x}, \boldsymbol{z})^{(k)*}}{||(\boldsymbol{x}, \boldsymbol{z})^{(k)*}||}, \tag{7}$$

where $(\boldsymbol{x}, \boldsymbol{z})^{(k)*}$ is the design point corresponding to the instantaneous performance function at the time instant $t_s^{(k)}$, and $\beta^{(k)} = ||(\boldsymbol{x}, \boldsymbol{z})^{(k)*}||$ is the corresponding distance form the origin to the design point. At this stage, it is assumed that this time instant $t_s^{(k)}$ is known. A specific criterion for its selection is discussed in Section 3.4. Regarding the determination of the design point, it can be carried out by using any optimisation algorithm or Advanced First Order and Second Moment (AFOSM) method [33], which is widely used in reliability analysis. Note that the proposed approach focuses on the time-variant problem where the instantaneous failure region is concentrated in one region, and only one design point exists. The treatment of problems with multiple regions or design points usually requires to account for several important directions [34]. However, this paper focuses on developing efficient strategy based on multiple Line sampling components with different important directions to solve the composite limit state associated with the time-variant problem.

Once the important direction has been identified, the next step of Line Sampling is exploring the failure domain by means of lines which are parallel to that important direction. This process is illustrated schematically in Fig. 1 in a two-dimensional problem. Suppose that a set of two-dimensional samples $\{(x, z)^{(j)},\ j = 1, 2, ..., N\}$ is generated (where N is the number of samples) according to the joint probability density function $f(x, z)$. Then, it is necessary to *explore* the lines that pass through each of the aforementioned samples and which are parallel to the important direction. In this context, to *explore* means that the intersection of each line with each instantaneous limit state function $g_z(x, t_i, z)$ $(i = 0, \ldots, n_t)$ should be determined. After finding the corresponding intersection points $(x, z)_{t_i}^{(j)*}$, $i = 0, \ldots, n_t$ associated with the instantaneous limit state function $g_z(x, t_i, z)$ and the line passing through the sample $(x, z)^{(j)}$, it is necessary to determine the distance value $c_{t_i}^{(j)*}$. Note that $c_{t_i}^{(j)*}$ measures the Euclidean distance between the hyperplane that passes through the origin of the standard normal space and which is orthogonal to the important direction and the intersection point $(x, z)_{t_i}^{(j)*}$. In practice, the intersection points can be determined by, e.g. three-point-second-order (TPSO) polynomial interpolation method [35]. To do this, the three values c_1, c_2 and c_3 that are associate with the distances along the line parallel to $\boldsymbol{\alpha}^{(k)}$ should be properly selected. In this paper, $c_1 = \beta^{(k)} - 3, c_2 = \beta^{(k)}$ and $c_3 = \beta^{(k)} + 3$

are used, which is deemed as appropriate after numerical verification. One can also increase the number of points on each line to improve the accuracy of estimating the intersection points.

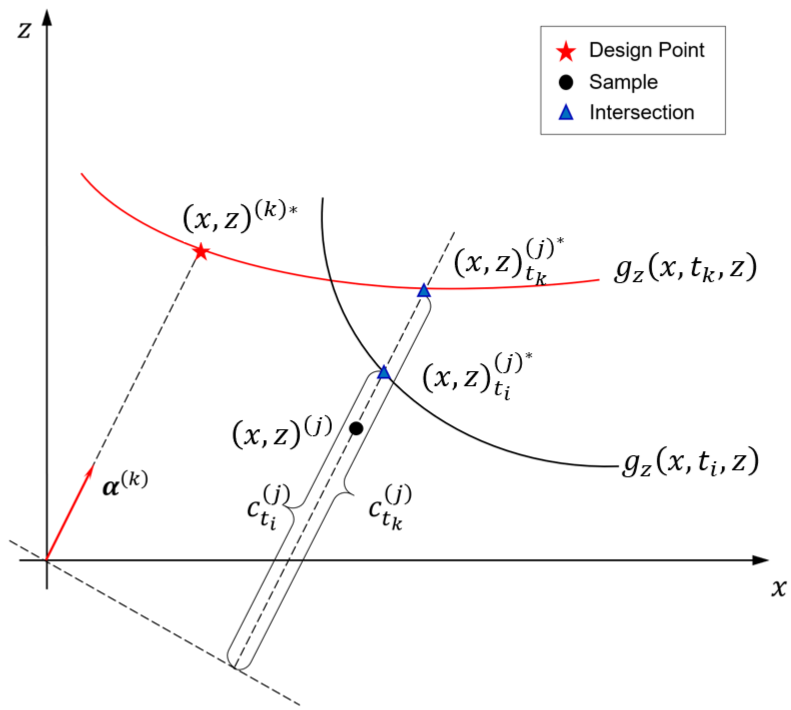

Figure 1: Schematic diagram of Line Sampling for the time-variant problem.

In summary, according to the reliability formula of time-variant series system, both Line Sampling and the concept of cumulative failure probability are adopted. The TFPF can be estimated as:

$$c^{(j)*}_{\min}(t_l) = \min(c^{(j)*}_{t_0}, \cdots, c^{(j)*}_{t_l}), \tag{8}$$

$$\hat{P}_{F,k}(t_l) = \frac{1}{N}\sum_{j=1}^{N} \Phi(-c^{(j)*}_{\min}(t_l)), \tag{9}$$

where $\hat{P}_{F,k}(t_l)$ is the TFPF component estimator based on $\boldsymbol{\alpha}^{(k)}$ with respect to k-th instantaneous LSF, $c^{(j)*}_{\min}(t_l)$ means the smallest value due to the series system property.

The variance and the coefficient of variation (C.o.V.) of this estimator are given as:

$$Var[\hat{P}_{F,k}(t_l)] \approx \frac{1}{N(N-1)}\sum_{j=1}^{N}\left(\Phi(-c^{(j)*}_{\min}(t_l)) - \hat{P}_{F,k}(t_l)\right)^2, \tag{10}$$

$$Cov[\hat{P}_{F,k}(t_l)] \approx \frac{\sqrt{Var[\hat{P}_{F,k}(t_l)]}}{\hat{P}_{F,k}(t_l)}, \tag{11}$$

Note that Line Sampling is carried out iteratively with a relative small number of samples N each time, and the corresponding important direction is actively updated in order to reach an overall convergence of the TFPF estimation. Additional details on the update of the important direction are discussed later on in Section 3.4.

3.3. Combination algorithm

In order to obtain the overall TFPF estimator $\hat{P}_F^{(m)}(t_l)$ in Eq. (4), an optimal combination algorithm is proposed to determine the weights function, $w_k(t_l)$, as introduced in Eq. (4). The performance of the combination approach is highly dependent on the weights and hence on the principle used to determine these weights. Since the C.o.V. of an estimator is the ratio between the standard deviation of an estimator and the mean estimator, and hence a good metric for its performance, it can be used to determine the weights function, that is, to find the optimal $w_k(t_l)$ that minimises the C.o.V. of $\hat{P}_F^{(m)}(t_l)$. Note that similar algorithms have also been reported for the estimation of failure probability in [8], improvement of Line sampling in [24] and also for calculating the failure probability function with respect to design distribution parameters of basic random variables in [25].

The optimal combination algorithm determines weights for component estimators which lead to the aggregate estimator $\hat{P}_F^{(m)}(t_l)$ with the smallest possible C.o.V. The corresponding optimal weights can be determined by:

$$w_k(t_l) = \frac{Cov\left[\hat{P}_{F,k}(t_l)\right]^{-2}}{\sum_{j=1}^{m} Cov\left[\hat{P}_{F,j}(t_l)\right]^{-2}} \quad (k = 1, \cdots, m), \tag{12}$$

The detailed derivation of Eq. (12) is discussed in Appendix A. Further substitution of Eq. (12) into Eq. (6) leads to the final C.o.V. of the estimate of TFPF, which is equal to:

$$Cov[\hat{P}_F^{(m)}(t_l)] = \frac{1}{\sqrt{\sum_{k=1}^{m} Cov^{-2}[\hat{P}_{F,k}(t_l)]}}. \tag{13}$$

When $Cov[\hat{P}_{F,k}(t_l)] \in [0, 1]$, it is easy to further deduce that:

$$Cov[\hat{P}_F^{(m)}(t_l)] \leq Cov[\hat{P}_{F,k}(t_l)], (k = 1, \cdots, m), \tag{14}$$

which means that the combined estimate will own the smallest C.o.V. in theory compared with the weighted components when the C.o.V.'s of TFPF components are less than 1.

3.4. Adaptive strategy

In this subsection, an active strategy is proposed to determine the support time instants $t_s^{(k)}(k=1,\ldots,m)$. For the first individual estimator $k=1$, $t_s^{(1)}$ can be arbitrarily selected within the time interval $[0,T]$, e.g., $t_s^{(1)}=0$, $T/2$, or T. Then, Line Sampling is carried out based on the important direction associated with the instantaneous performance function at time $t_s^{(k)}$. Note that the selection of $t_s^{(k)}$ affects the efficiency of the proposed approach and should therefore be performed with care. As such, a novel way to determine the support time instants in an active learning fashion is developed in the following.

Since C.o.V. is a good characteristic quantity to monitor the convergence of the probability estimator, it can be used as a learning function to determine the next support time instant. Specifically, the time instant that has the largest value of C.o.V. should be chosen as the next support time instant. Suppose the k-th estimator of the TFPF $\hat{P}_{F,k}(t)$ has been calculated using Line Sampling, and the C.o.V. of the estimator is obtained according to Eq. (13), then the next support time instant can be obtained by solving the following optimisation problem:

$$\begin{aligned} &\text{Find} \quad t_l = t_s^{(k+1)} \\ &\text{Max} \quad Cov[\hat{P}_F^{(k)}(t_l)] = \sqrt{\textstyle\sum_{i=1}^{k} w_i^2(t_l) Cov^2[\hat{P}_{F,i}(t_l)]} \\ &\text{s.t.} \quad t_0 \le t_l \le t_{n_t} \end{aligned} \quad . \tag{15}$$

Inspection of Eq. (15) reveals that the next support time instant $t_s^{(k+1)}$ should be the one having the largest C.o.V. value. It is expected that the identified time instant has the largest potential for improving the convergence of the estimates of TFPF by carrying out a component Line Sampling according to the importance direction associated with $t_s^{(k+1)}$. Note that this optimisation problem does not involve any evaluation of the performance function, and it is actually just a single-dimensional optimisation problem. Thus it can be readily solved by adopting any appropriate optimisation algorithm. Moreover, it is not necessary to obtain the exact solution of the optimisation problem in Eq. (15), as the time $t_s^{(k+1)}$ that is being identified is just used to establish an important direction and in several cases, Line Sampling is not so sensitive with respect to that important direction. As the optimisation problem in Eq. (15) can be solved with negligible numerical cost, it is solved using random search with Monte Carlo simulation.

The adaptive strategy for selecting time instants $t_s^{(k)}$ is repeated until a convergence criterion is fulfilled. This convergence criterion is established as $\mathrm{Max}_{l=0,\ldots,n_t}\{Cov[\hat{P}_F^{(k)}(t_l)]\} \le C^{\mathrm{tol}}$, where C^{tol} is a predefined threshold value, e.g, $C^{\mathrm{tol}}=0.1$ can be chosen for general cases.

In conclusion, the proposed approach utilises the information of C.o.V. at each step to adaptively select the time instant for which Line Sampling is run (with its corresponding important direction). As the probability estimator is simulation-based, the accuracy can be guaranteed as the simulation proceeds until satisfying the convergence condition. In the following numerical applications, it is shown that the proposed approach exhibits excellent efficiency, and that the proposed Adaptive Combined Line Sampling (ACLS) is highly rewarding.

3.5. Summary of the proposed approach

The proposed approach for estimating the time-variant failure probability function (TFPF) is summarized as follows, as well as shown in Fig. 2.

1. Choose the initial support time instant $t_s^{(1)}$. Generally, the midpoint of the time interval $[0, T]$ can be chosen, i.e., $t_s^{(1)} = T/2$.
2. Stochastic processes are represented by spectral decomposition, and the equivalent composite performance functions are obtained.
3. Based on the current support time instant $t_s^{(k)}$, identify the design point $(\boldsymbol{x}, \boldsymbol{z})^{*(k)}$ and set the important direction $\boldsymbol{\alpha}^{(k)}$ by means of Eq. (7). Generate samples $(\boldsymbol{x}, \boldsymbol{z})^{(j)}, j = 1, \ldots, N$. Calculate the component probability estimator given in Eq. (9) and its C.o.V. with Eq. (11).
4. Apply the combination algorithm to produce an updated estimator of TFPF as given by Eqs. (4) and (12), as well as its C.o.V. in Eq. (13).
5. Determine the next support time instant $t_s^{(k+1)}$ by solving the optimisation problem given in Eq. (15).
6. Repeat steps 3 to 5 until the convergence criterion, $\max\{Cov[\hat{P}_F^{(k)}(t)]\} \leq C^{\text{tol}}$, is reached.

4. Examples

In this section, examples are given to illustrate the performance of the proposed Adaptive Combination Line Sampling (ACLS) method in terms of accuracy and efficiency. Direct Monte Carlo simulation (MCS), Importance Sampling (IS)[36], Line Sampling (LS) [6] and Advanced Line Sampling (ALS) [7] are used for comparison. The unit coefficient of variation Δ is calculated in all examples considered [9]. This unit coefficient of variation is – in theory – invariant to the accuracy achieved and the computational effort spent, where smaller values of Δ correspond to

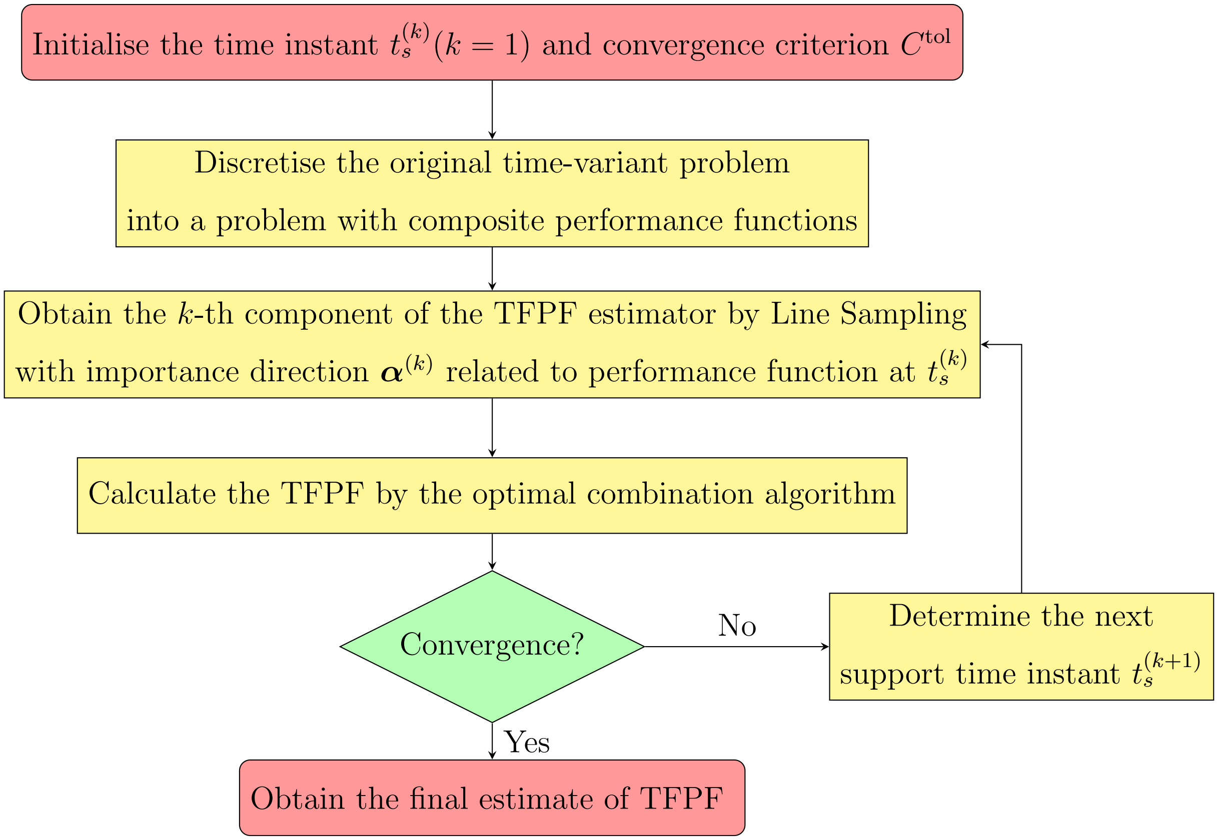

Figure 2: Procedure of the proposed ACLS method

a higher computational efficiency. Note that the three-point quadratic interpolation is used to obtain the intersections for LS, ALS and ACLS in this contribution.

For Examples 1 and 2, a time period of $[0, 20]$ years is considered, and a time interval $\Delta t = 2$ year is adopted to discretise the time interval in the calculation. For example 3, a time period of $[0, 10]$ years with the time interval $\Delta t = 1$ years is considered. Also, the number of identified dominating eigenfunctions in K-L expansion is chosen as $n_{kl} = 5$, which has been found to be reasonable for all these examples.

4.1. Example 1: Test example

The following performance function with two random variables and a stochastic process is considered in this example:

$$g(\boldsymbol{x}, t, \boldsymbol{y}(t)) = 17 - x_1^2 + 2x_2 \exp(-0.1t) - 5F(t) \tag{16}$$

where $\boldsymbol{x} = [x_1, x_2]$ is the vector of random variables; $\boldsymbol{y}(t) = F(t)$ is a stochastic load which is modelled as a stationary Gaussian random process, and the auto-correlation coefficient function is of the squared exponential type, which is given as:

$$\rho_F(t_1, t_{l+1}) = \exp\left\{-0.05(t_{l+1} - t_l)^2\right\}. \tag{17}$$

The information of these inputs is listed in Table 1.

Table 1: Information of variables and parameters for two-dimension nonlinear example (Example 1)

Parameter	Distribution	Mean	Standard deviation	Auto-correlation coefficient function
x_1	Normal	2.6	0.26	–
x_2	Normal	5	0.5	–
$F(t)$	Gaussian process	2	0.2	Eq. (17)

In this example, the number of variables representing $F(t)$ in K-L expansion is 5, thus the final total dimension of the reliability problem $(\boldsymbol{x}, \boldsymbol{z})$ is 7. The proposed approach is applied with $N = 100$ samples (lines) in each individual run of Line Sampling for calculating the component probability, and the convergence criterion $C^{\text{tol}} = 0.2$ is selected. In this context, the adaptive strategy is carried out for $m = 3$ rounds until convergence is achieved, and thus a total of $N_T = 300$ samples are used. The traditional LS, IS and ALS are also applied with the same sampling number $N_T = 300$. And IS and LS are carried out based on the design point and the important direction corresponding to the instantaneous LSF at time instant $t_{mid} = T/2$, respectively. In addition, Direct MCS is also applied with $N = 10^7$ samples, and its results are seen as the reference values.

Fig. 3 plots the curves of TFPF and C.o.V. with respect to time t during the intermediate process of the proposed approach. It can be seen that, in the initial round $k = 1$ of proposed method, the corresponding TFPF result owns considerable error when $t \in [0, 5]$, the C.o.V over these time instants exceeds 0.2. When including new support time instants, however, the accuracy of TFPF estimator is improved and the C.o.V curve becomes smoother and smaller. At the third iteration, the C.o.V is less than 0.2 and the result obtained from ACLS method is consistent with the exact value from MCS. This illustrates the effectiveness and accuracy of the proposed method.

The results of TFPF obtained by different methods (LS, IS, ALS and ACLS) with the same total number of samples N_T =300 are plotted in Fig. 4. It can be seen that the results that are obtained by these methods agree very well with each other. Also the corresponding C.o.V. of the proposed ACLS is smaller than those of LS, IS and ALS over most parts of the considered time period, especially in $t \in [0, 5]$. This means that the proposed approach seems to reasonably

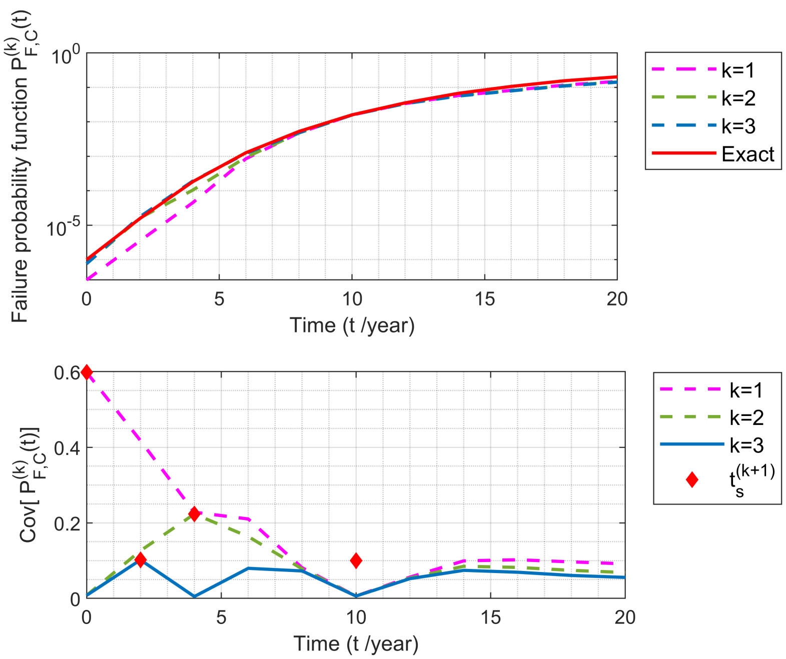

Figure 3: Evolution of TFPF result obtained by the proposed approach (Example 1).

allocate samples in order to obtain satisfactory results over the whole time domain, due to the adaptive strategy adopted in the proposed approach.

To investigate the performance of the proposed method more clearly, the same stopping criterion is used for ACLS, ALS, IS, and LS. Fig. 5 shows the total number of samples N_T, and total number of function calls N_{call} (including the interpolation calculation in line sampling, as well as the design point solving) used by different methods under the same $C^{\text{tol}} = 0.2$. It can be seen from the figure that, while the proposed approach required only $N = 300$ simulated samples (lines) to achieve $\max\{Cov[\hat{P}_F^{(k)}(t)]\} \leq C^{\text{tol}} = 0.2$, far more samples are needed by LS (about 120 times of that by ACLS) and by ALS (about 20 times), respectively. In terms of total number of calls, the proposed ACLS method is more efficient than other methods (about only 1/104 of that by LS, 1/274 of that by IS and 1/18 of that by ALS). Hence, it can be drawn that the proposed approach can produce a satisfactory TFPF estimate in a more efficient way.

For further comparison, the numbers of samples used by different methods with respect to the stopping criterion value C^{tol} are shown in Fig. 6. It is apparent from the figure that the numbers of samples decrease for these methods as the C^{tol} increases. Moreover, LS, IS and ALS demand more samples than ACLS to meet the same convergence criterion. It can be concluded that, in terms of efficiency, the proposed ACLS method is certainly superior to the LS, IS and the ALS. However, this last conclusion must be weighed against the fact that ACLS is specifically developed

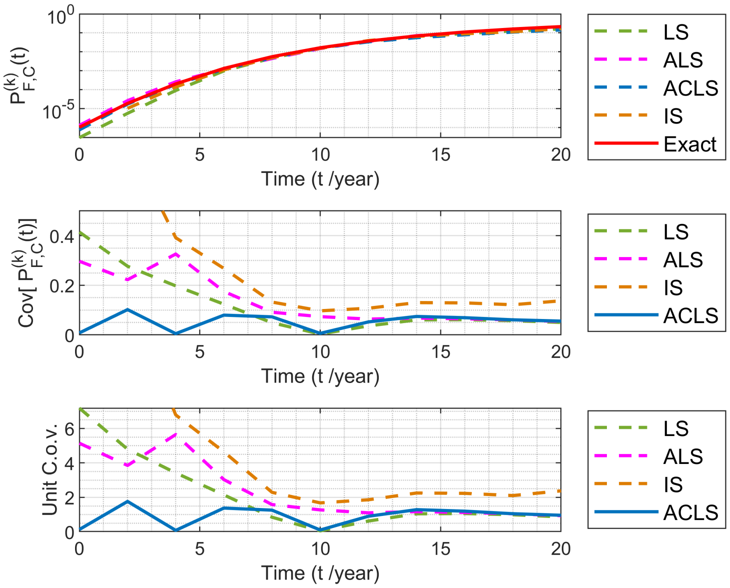

Figure 4: TFPF results obtained by different methods using the same number of samples $N_T = 300$ (Example 1).

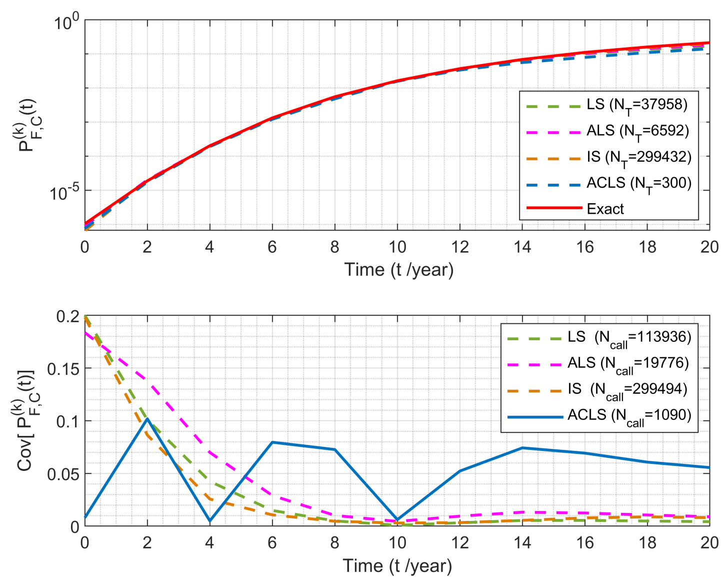

Figure 5: TFPF results obtained by different methods using the same convergence criterion C^{tol} value (Example 1).

to address time-variant reliability problems.

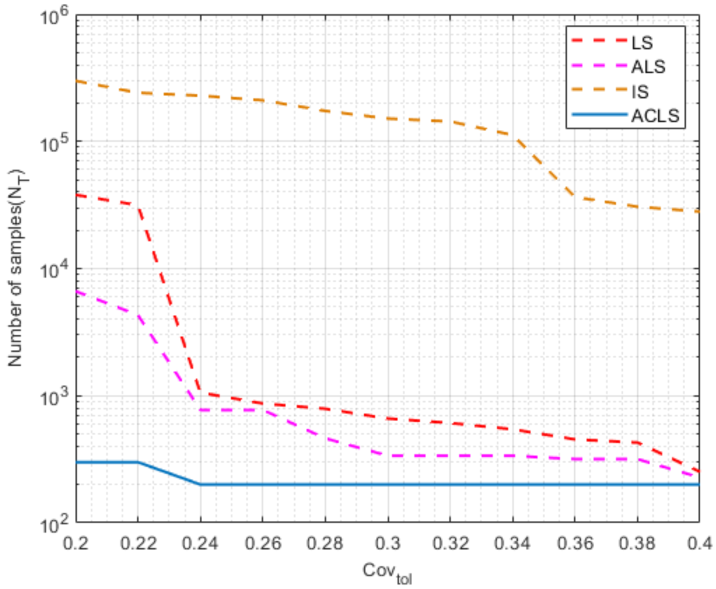

Figure 6: Total number of samples used by different methods with respect to the convergence criterion C^{tol} value (Example 1).

The TFPF results obtained by the proposed method with different stopping criteria C^{tol} and a fixed $N = 100$ are depicted in Fig. 7. It shows that, the results from $C^{tol} = 0.05$ to $C^{tol} = 0.2$ all match well with the reference value obtained by MCS. However, it should also be noted that the smaller C^{tol} is, the higher computational effort the method demands.

The performance of ACLS method under different initial settings (i.e. initial support time instant) is depicted in Fig. 8. Three initial support time instants $t_s^{(1)} = t_0$, $t_s^{(1)} = t_{mid} = T/2$, and $t_s^{(1)} = t_{max} = T$ are considered, respectively. Note that N_T represents the total number of sampling lines used in all iterations, while N_{call} represents the number of performance function evaluations. The results show that, the number of iterations decreases as N increases for each initial setting, however N_T as well as N_{call} have an increasing trend, though fluctuations exist. Thus, the selection of N clearly affects the efficiency of proposed method and hence, N should be properly selected. Generally, N could be selected such that $Cov[\hat{P}_F^{(1)}(t_s^{(1)})] \leq C^{\mathrm{tol}}$ is achieved at least.

4.2. Example 2: A steel beam in bending

A steel beam in bending shown in Fig. 9 is considered in this example, which is taken (in revised form) from [4]. The size of this beam is 5 m (length) $\times$ 0.2 m (width b_0) $\times$ 0.04 m (height

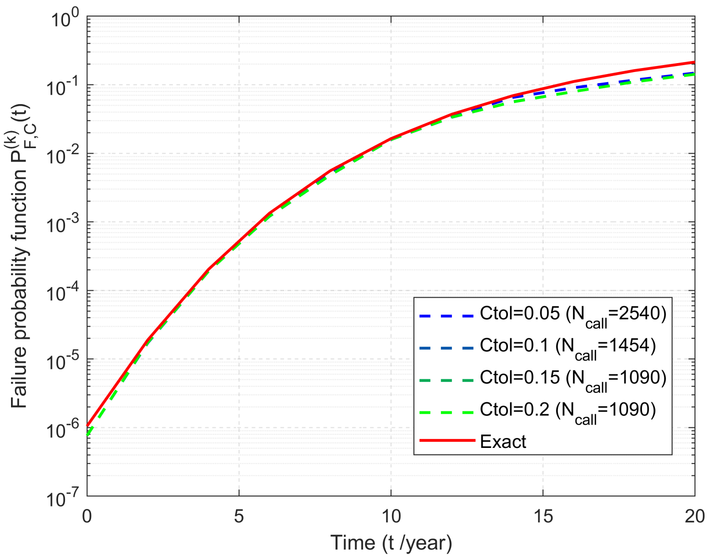

Figure 7: TFPF results obtained by the proposed approach with different C^{tol} (Example 1).

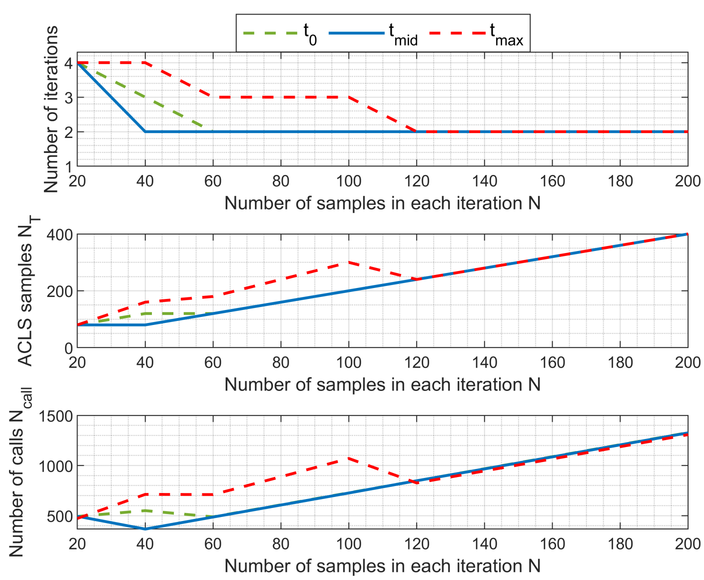

Figure 8: Performance of proposed method starting for different initial support time instants (Example 1).

h_0). It is assumed that the beam corrodes in time, and the dependency of the dimensions to time can be expressed as

$$b(t) = b_0 - 2\kappa t; h(t) = h_0 - 2\kappa t \tag{18}$$

where parameter $\kappa = 0.03$ mm/ year controls the corrosion kinetics. This beam is subjected to a dead load $p = \rho_{st} b_0 h_0$ where $\rho_{st} = 78.5 kN/m^3$ is the steel force density, as well as a point load $F(t)$ applied at the mid span. The bending moment at mid-span associated with dead- and point loads reads:

$$M(t) = \frac{F(t)L}{4} + \frac{\rho_{st} b_0 h_0 L^2}{8} \tag{19}$$

Considering that the bending moment should be less than the ultimate bending moment corresponding to the appearing of a plastic hinge in the section, the performance function of the beam is given by:

$$G(\boldsymbol{x}, t, F(t)) = \frac{b(t)h^2(t)f_y}{4} - \left(\frac{F(t)L}{4} + \frac{\rho_{st} b_0 h_0 L^2}{8}\right) \tag{20}$$

where $\boldsymbol{x} = [f_y, b_0, h_0]$ is the vector of random variables; f_y is the steel yield stress; $F(t)$ is the load which is modelled as a stationary Gaussian random process, and the auto-correlation coefficient function is of exponential squared type, which is given as:

$$\rho_F(t_1, t_{l+1}) = \exp\left\{-0.05(t_{l+1} - t_l)^2\right\} \tag{21}$$

The information of these inputs are listed in Table 2. The time interval under consideration is $[0, 20]$ years.

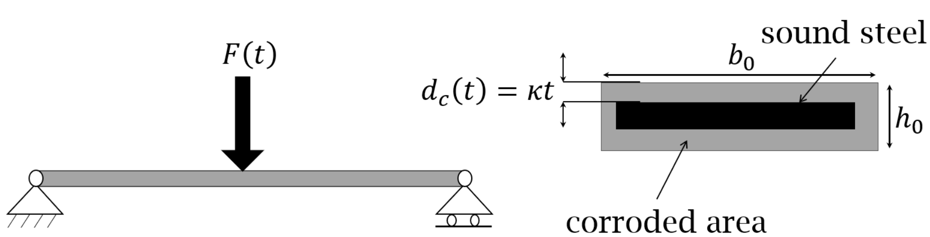

Figure 9: Corroded bending beam

In this example, the proposed approach is applied with $N = 100$, and the convergence criterion $C^{\text{tol}} = 0.2$ is selected. In this context, the adaptive strategy is carried out for $m = 4$ rounds to achieve convergence, and thus a total of $N_T = 400$ samples are used. The traditional LS, IS and ALS are also applied with the same number of samples. In addition, MCS is applied for comparison which is seen as the exact value.

Table 2: Information of random variables and parameters of corroded steel beam in bending (Example 2)

Parameter	Distribution	Mean	Standard deviation	Autocorrelation coefficient function
f_y/MPa	Lognormal	240	24	–
b_0/m	Lognormal	0.2	0.01	–
h_0/m	Lognormal	0.04	0.004	–
$F(t)$/N	Gaussian process	3500	700	Eq. (21)

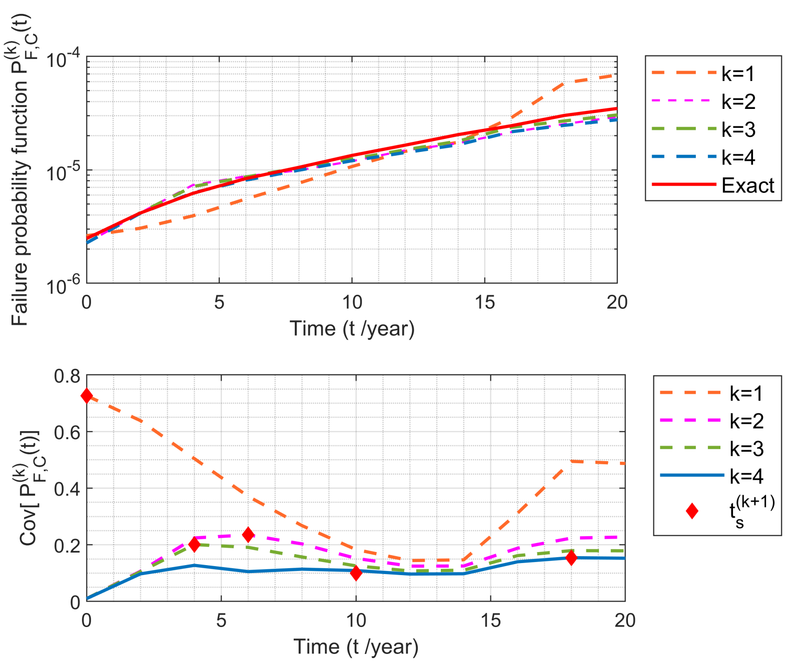

Figure 10: Intermediate TFPF results of the proposed ACLS approach (Example 2).

Fig. 10 shows the intermediate TFPF results of the proposed approach. It can be seen that, in the first round $k = 1$, the TFPF result obtained has considerable error, e.g., when $t \in [16, 20]$ years and the corresponding C.o.V. is also bigger than 0.2. However, after the fourth iteration, the C.o.V. is always smaller than 0.2, leading to an estimate of the time-variant failure probability that compares very well with the reference. This demonstrates the effectiveness of the ACLS method proposed in this paper.

The results of ACLS with different settings of N and fixed $C^{tol} = 0.2$ are shown in Fig. 11 to investigate the effect of the number of samples N on the accuracy. The proposed method was run repeatedly and independently for 100 times. The corresponding mean values of TFPF estimates, the relative errors and N are shown in the figure. From a statistical viewpoint, it can be seen that the accuracy of the proposed ACLS increases with the increasing of N. However, the gain in accuracy partly comes at the expense of an increase of computational cost which can be seen from the growing of N_{call}.

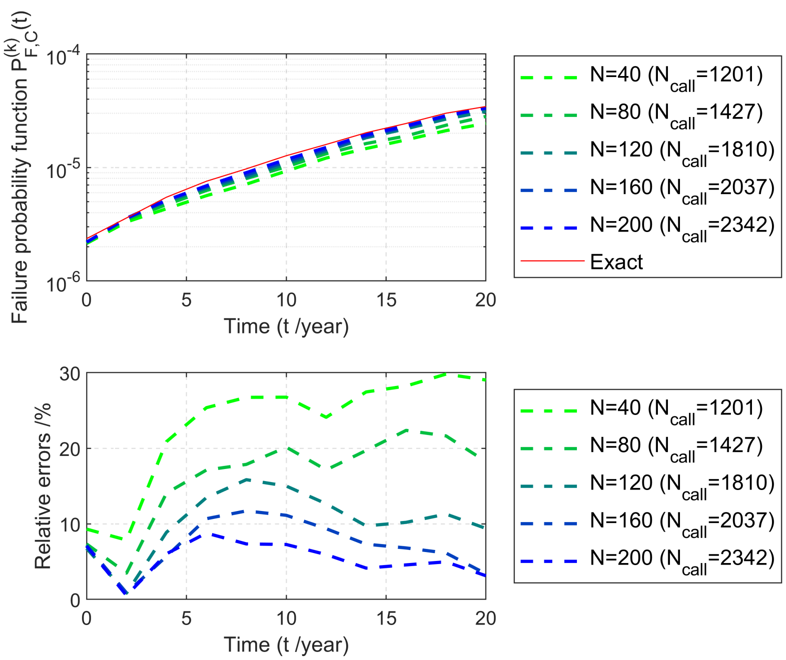

Figure 11: TFPF result obtained by the proposed approach with different N and a fixed $C^{tol} = 0.2$ (Example 2).

Fig. 12 depicts the TFPF results by traditional LS, IS, ALS and ACLS when the same number of samples is considered. As it can be seen from the figure, traditional LS and IS produces a TFPF estimate with considerable error, and the corresponding C.o.V.'s for LS, IS and ALS are greater than 0.2 when $t \in [0, 5]$ year. In contrast, the proposed ACLS can produce an accurate estimate which is consistent with the exact values, while ensuring that the associated C.o.V. is

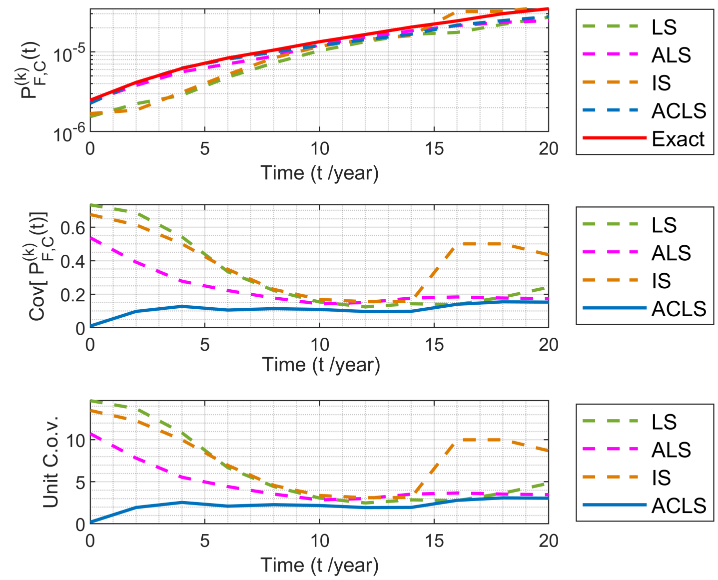

Figure 12: TFPF results obtained by different methods when the same number of samples is used (Example 2).

smaller than 0.2. This shows the advantage in efficiency and performance of the proposed ACLS method.

To further investigate the performance, LS, IS, ALS and the proposed ACLS are carried out under the same stop criterion of $C^{\mathrm{tol}} = 0.2$, and the corresponding results are shown in Fig. 13. It can be seen that, while the obtained TFPF results by these four methods are consistent with the exact values, the number of simulated samples used to achieve the convergence for these four methods is quite different, as noted from the figure, i.e., $N_T = 3463$ for LS, $N_T = 55261$ for IS, $N_T = 1260$ for ALS and $N_T = 400$ for the proposed ACLS method. Accordingly, the number of function calls is as follows: $N_{call} = 10495$ for LS, $N_{call} = 55367$ for IS, $N_{call} = 3780$ for ALS and $N_{call} = 1619$ for the proposed ACLS method. That is, the proposed approach needs less function calls to reach the convergence, nearly 1/6 of those by LS, 1/34 of those by IS, or 1/2 of those by ALS.

4.3. Example 3: turbine blade

This example considers a jet engine turbine blade, as shown in Fig. 14. This blade has interior cooling ducts, through which the flow of cool air maintains the temperature of the blade within a prescribed limit. The turbine is a radial array of blades made of nickel alloys. These alloys resist extremely high temperatures of the gases. At such temperatures, the material expands

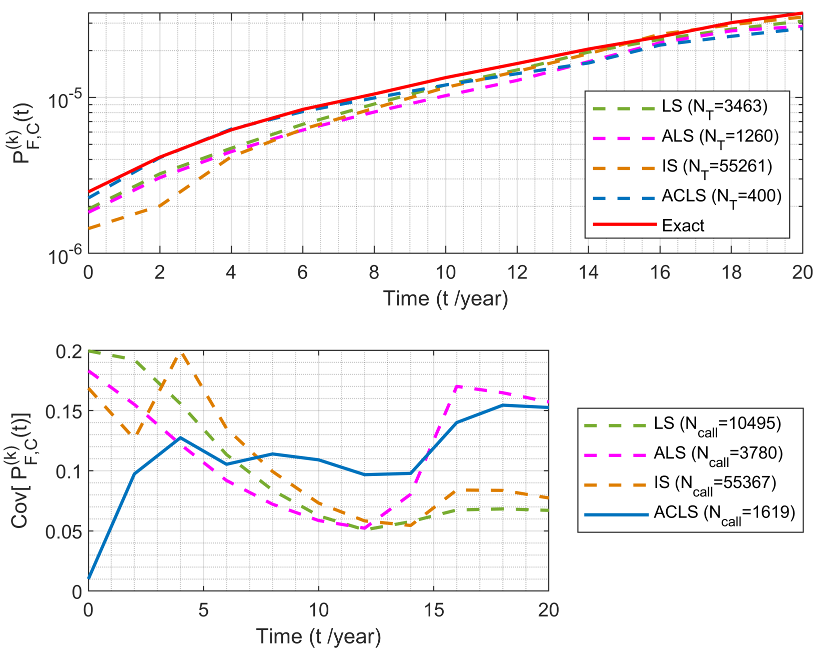

Figure 13: TFPF results of different methods under the same convergence criterion of C.o.V. (Example 2).

significantly, producing mechanical stress in the joints and significant deformations. Failure is in this case defined as the maximum von Mises stress of the structure exceeding the allowable value $\sigma_a = 1.5$GPa, and the corresponding performance function is:

$$g(\boldsymbol{x}, t, \boldsymbol{Y}(t)) = \sigma_a \exp(-0.03t) - \sigma_{max}(\boldsymbol{x}, \boldsymbol{y}(t)), \tag{22}$$

where $\sigma_{max}(\boldsymbol{x}, \boldsymbol{y}(t))$ is the maximum von Mises stress of the blade caused be the combination of thermal and pressure effects; $\boldsymbol{x} = [E, \gamma_{CTE}, \lambda, K_{app}, T_1, T_2]$ is the vector of basic random variables; E, γ_{CTE}, λ and K_{app} are the Young's modulus, coefficient of thermal expansion, Poisson's ratio and the thermal conductivity for nickel-based alloy (NIMONIC 90), respectively; T_1 is the temperature of the interior cooling air and T_2 is temperature on the pressure and suction sides; $\boldsymbol{y}(t) = [F_1(t), F_2(t)]$, where $F_1(t)$ and $F_2(t)$ are the pressure loads on the pressure and suction sides of the blade which are caused by the high-pressure gas surrounding the sides of the blade. Input random parameters and distribution parameters of random processes are shown in Table 3. Parameters modelled with a normal distribution which must be within a prescribed range due to physical reasons are truncated.

In this example, the final dimension of the vector $(\boldsymbol{x}, \boldsymbol{z})$ is 16 as the number of K-L expansion terms $n_{kl} = 5$ is considered. The proposed approach is applied with $N = 100$, and the convergence

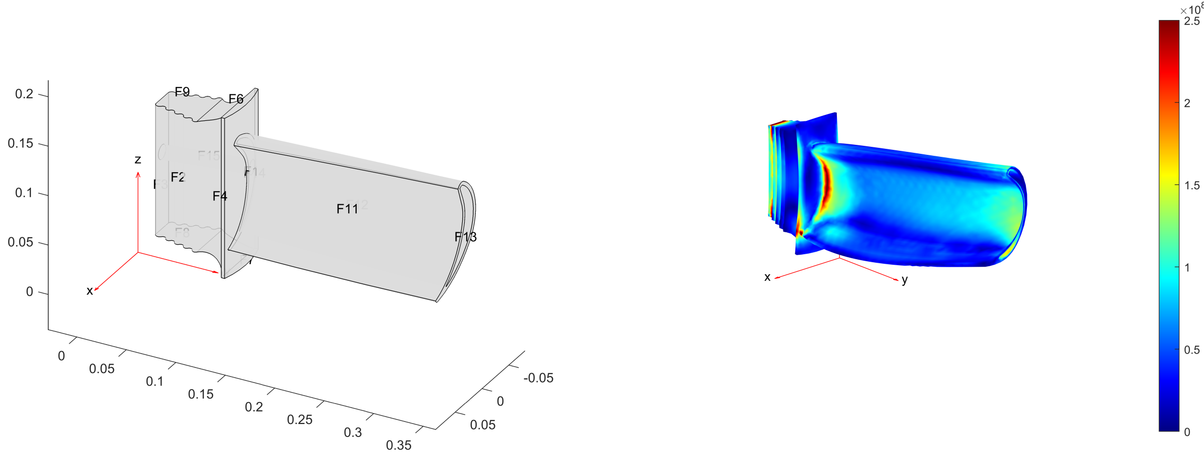

Figure 14: Geometry and von Mises stress of a turbine blade.

Table 3: Information of random variables and parameters (Example 3)

Variables	Distribution	Mean	Standard deviation	Autocorrelation function
E/Pa	Normal	225×10^9	223×10^8	-
$\gamma_{CTE}/(1/\mathrm{K})$	Normal	13×10^{-6}	13×10^{-7}	-
λ	Normal	0.27	0.027	-
$K_{app}/(\mathrm{W}/(\mathrm{m} \cdot \mathrm{K}))$	Normal	11.5	1.15	-
$T_1/°\mathrm{C}$	Normal	150	15	-
$T_2/°\mathrm{C}$	Normal	1000	100	-
$F_1(t)$/Pa	Gaussian process	5×10^5	1×10^5	$\exp\left\{-(\frac{t_{l+1}-t_l}{2})^2\right\}$
$F_2(t)$/Pa	Gaussian process	2×10^5	4×10^4	$\exp\left\{-(\frac{t_{l+1}-t_l}{2})^2\right\}$

criterion $C^{\text{tol}} = 0.05$ is selected. In this context, the adaptive strategy is carried out for $m = 2$ iterations until convergence is achieved, and thus a total of $N_T = 200$ lines are used. The traditional LS, IS and ALS are also applied with the same number of simulated samples. In addition, Direct MCS is also applied for comparison, which is deemed as the exact value.

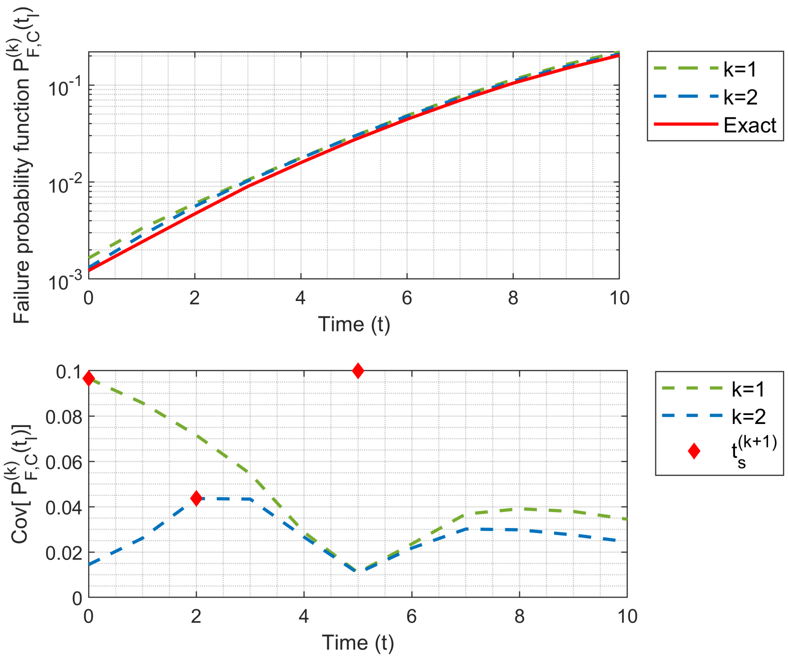

Figure 15: TFPF results varying with the number of iteration rounds (Example 3).

Fig.15 shows the results obtained by the proposed ACLS approach with respect to the number of iteration steps k. By observing the results and the coefficient of variation in the figure, it can be found that, in the first iteration, the estimated results have slight deviation from the reference values. At the same time, the maximum coefficient of variation is close to 0.1. In this case, the adaptive strategy selects the support time of next iteration to be at the time instant $t = 0$ where the coefficient of variation is the largest. After only one additional iteration, the largest C.o.V. is reduced below 0.05, and the C.o.V curve with respect to time tends to be flat. The above analysis verifies the effectiveness of the proposed ACLS method.

Fig. 16 shows the TFPF results and C.o.V. by the proposed ACLS compared with LS, IS and ALS methods. As shown in the figure, with the same total number of samples, all methods produce accurate estimates. Regarding the coefficient of variation, the maximum coefficient of variation of the LS method is more than 0.05, and that of the advanced line sampling method and IS method exceeds 0.1, while the C.o.V. curve by the proposed ACLS method is below 0.05 over the whole interval $t \in [0, 10]$ year.

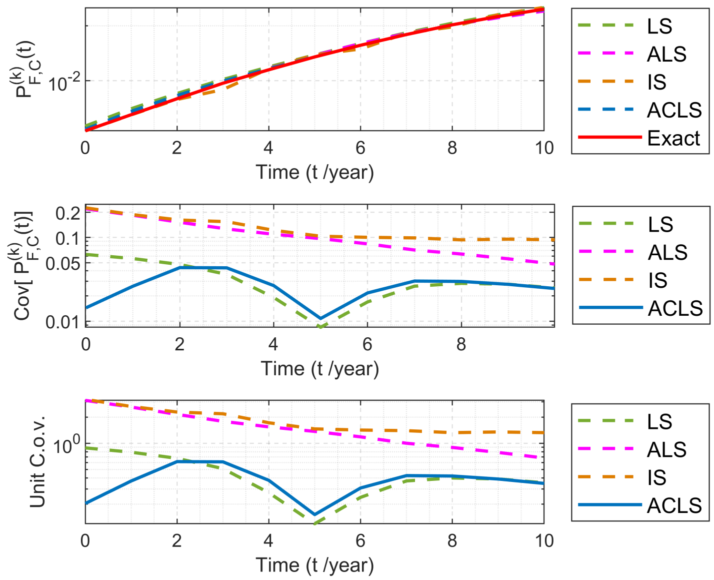

Figure 16: TFPF results obtained by different methods using the same number of samples (Example 3).

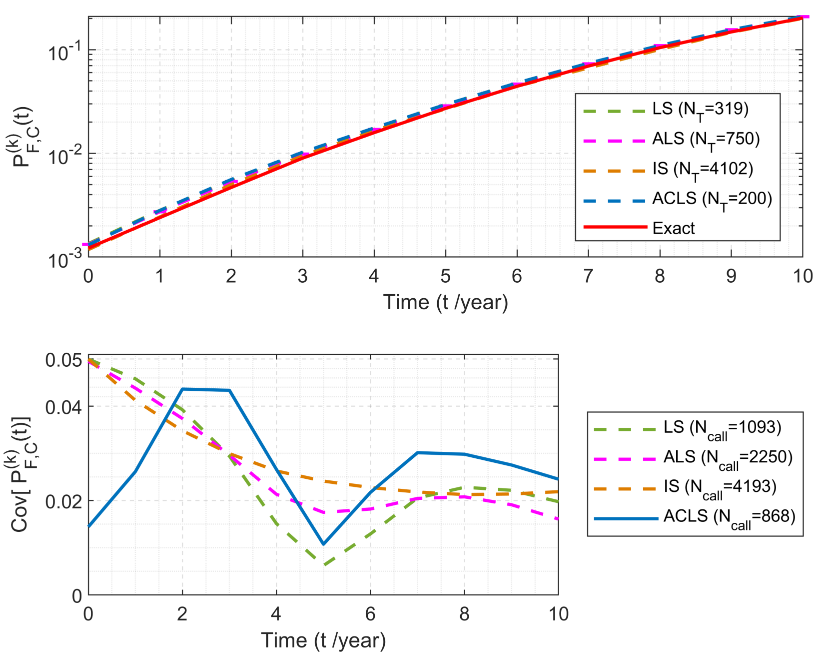

Figure 17: TFPF results obtained by different methods using the same convergence criterion C^{tol} value (Example 3).

Fig. 17 shows the results by different methods with the same convergence criterion $C^{\text{tol}} = 0.05$. It can be seen that, LS, ALS and IS used 319, 750 and 4102 samples to reach the stopping criterion, respectively, while ACLS used just 200 samples to do so. Besides, the total number of function calls needed by ACLS is approximately 4/5 of that by LS, 1/5 of that by IS, and 2/5 of that by ALS, respectively.

5. Conclusions

A new efficient Adaptive Combined Line Sampling (ACLS) approach has been proposed to estimate the time-variant failure probability function of structures. This approach follows the 'composite limit states' concept which transforms the time-variant problem into a series system through discretisation. An adaptive strategy and an optimal combination algorithm have been proposed to solve the time-variant failure probability function (TFPF) efficiently. The original contribution of this work is that the convergence of the overall TFPF (measured in a maximum of C.o.V. over the time span) can be ensured by selecting support points in an active fashion. Numerical and practical examples have been presented to show the advantages of the proposed approach with respect to existing techniques. It is observed that the proposed approach shows a high efficiency in the sense of obtaining the TFPF for a given convergence criterion.

Despite progress in the proposed method, limitations still remain. Since the accuracy of the method highly depends on the accuracy in the determination of the most probable point, the LS component estimators could produce errors, potentially compromising the accuracy of the obtained results. Also, special attention should be paid to the problem with multiple important directions (failure regions) where underestimation may occur if any failure region is neglected. Additionally, to perform LS component estimators, it is necessary to transform the limit state function into the standard normal space. Furthermore, due to the small sample size N in each iteration, using LS estimators to deal with a high-dimensional and highly non-linear LSF can lead to noisy and biased results. Through the validation of three examples, the proposed ACLS method is applicable for moderate nonlinear and moderate dimensional problems.

Future work will concentrate on the combination of the presented algorithms with Advanced Line Sampling (ALS) [7] and active learning LS methods [35] instead of Line Sampling (LS) to avoid the calculation of design point(s) and to further alleviate the computational burden. Efforts will also be made to apply the proposed approach to problems involving non-stationary/non-

Gaussian processes. Another future research task is to apply the proposed approach to systems involving multiple performance functions.

CRediT authorship contribution statement

Xiukai Yuan: Conceptualization, Methodology, Software, Validation, Writing - original draft, Funding acquisition. Weiming Zheng: Methodology, Software, Writing - original draft. Chaofan Zhao: Software, Writing - original draft. Marcos A. Valdebenito: Methodology, Supervision, Writing - original draft, Writing - review & editing. Matthias Faes: Writing - review & editing. Yiwei Dong: Writing - review & editing, Funding acquisition.

Declaration of competing interest

The authors declare that they have no known competing financial interests or personal relationships that could have appeared to influence the work reported in this paper.

Acknowledgements

Xiukai Yuan would like to acknowledge financial support from the Aeronautical Science Foundation of China (Grant No. ASFC-20170968002). Yiwei Dong acknowledges the financial support from the Aeronautical Science Foundation of China (Grant No. ASFC-20170368001), and the National Major Science and Technology Projects of China (Nos. J2019-III-0008, J2019-VII-0013-0153).

Appendix A. Selection of weights for minimising C.o.V.

This Appendix shows that the optimal weights based on minimising the C.o.V. are given by Eq. (12). Note that similar principles for combination algorithms have been used in [8, 24, 25]. However, it is worth to point out that in this paper, this algorithm is applied to solve the time-variant failure probability function, which is distinct with respect to the aforementioned contributions. As minimising the $Cov[\hat{P}_F^{(m)}(t)]$ is equal to minimising the $Cov^2[\hat{P}_F^{(m)}(t)]$, then the optimisation problem of minimising the C.o.V. to find the optimal weights is recast as follows:

$$\begin{aligned} \min \quad & Cov^2[\hat{P}_F^{(m)}(t)] = \sum_{k=1}^{m} w_k^2(t) Cov^2\left[\hat{P}_{F,k}(t)\right] \\ s.t. \quad & \sum_{k=1}^{m} w_k(t) = 1 \end{aligned} \tag{A.1}$$

Using the Lagrange multipliers method, the Lagrangian of the problem of Eq. (A.1) can be expressed as

$$L(\boldsymbol{w},\lambda)=\sum_{k=1}^{m} w_k^2(t)Cov^2\left[\hat{P}_{F,k}(t)\right]+\lambda\left(\sum_{k=1}^{m} w_k(t)-1\right) \tag{A.2}$$

The first-order necessary conditions for optimality read:

$$\begin{aligned}\frac{\partial L(\boldsymbol{w},\lambda)}{\partial w_k(t)}&=0\\ \frac{\partial L(\boldsymbol{w},\lambda)}{\partial \lambda}&=0\end{aligned} \tag{A.3}$$

Solving this system of equations will result in the following expressions

$$\begin{aligned}w_k(t)&=-\frac{\lambda}{2}Cov^{-2}\left[\hat{P}_{F,k}(t)\right]\\ \lambda&=-\frac{2}{\sum_{k=1}^{m}Cov^{-2}\left[\hat{P}_{F,k}(t)\right]}\end{aligned} \tag{A.4}$$

which leads to:

$$w_k(t)=\frac{Cov^{-2}\left[\hat{P}_{F,k}(t)\right]}{\sum_{j=1}^{m}Cov^{-2}\left[\hat{P}_{F,j}(t_l)\right]}\quad (k=1,\ldots,m) \tag{A.5}$$

Since the objective function is convex (quadratic in w) and the constraint is affine, the result of Eq. (A.5) is the global optimum.

References

[1] D. Straub, R. Schneider, E. Bismut, H.-J. Kim, Reliability analysis of deteriorating structural systems, Structural Safety 82 (2020) 101877.

[2] C. Jiang, X. Huang, X. Han, D. Zhang, A time-variant reliability analysis method based on stochastic process discretization, Journal of Mechanical Design 136 (2014).

[3] Z. P. Mourelatos, M. Majcher, V. Pandey, I. Baseski, Time-dependent reliability analysis using the total probability theorem, Journal of Mechanical Design 137 (2015).

[4] C. Andrieu-Renaud, B. Sudret, M. Lemaire, The phi2 method: a way to compute time-variant reliability, Reliability Engineering & System Safety 84 (2004) 75–86.

[5] X.-Y. Zhang, Z.-H. Lu, S.-Y. Wu, Y.-G. Zhao, An efficient method for time-variant reliability including finite element analysis, Reliability Engineering & System Safety 210 (2021) 107534.

[6] H. Pradlwarter, G. I. Schuëller, P.-S. Koutsourelakis, D. C. Charmpis, Application of line sampling simulation method to reliability benchmark problems, Structural safety 29 (2007) 208–221.

[7] M. de Angelis, E. Patelli, M. Beer, Advanced line sampling for efficient robust reliability analysis, Structural Safety 52 (2015) 170–182.

[8] M. A. Shayanfar, M. A. Barkhordari, M. Barkhori, M. Rakhshanimehr, An adaptive line sampling method for reliability analysis, Iranian Journal of Science and Technology, Transactions of Civil Engineering 41 (2017) 275–282.

[9] S. K. Au, J. L. Beck, First excursion probabilities for linear systems by very efficient importance sampling, Probabilistic Engineering Mechanics 16 (2001) 193–207.

[10] M. A. Misraji, M. A. Valdebenito, H. A. Jensen, C. F. Mayorga, Application of directional importance sampling for estimation of first excursion probabilities of linear structural systems subject to stochastic Gaussian loading, Mechanical Systems and Signal Processing (2020) 106621.

[11] S. K. Au, J. L. Beck, Estimation of small failure probabilities in high dimensions by subset simulation, Probabilistic Engineering Mechanics 16 (2001) 263–277.

[12] H.-S. Li, T. Wang, J.-Y. Yuan, H. Zhang, A sampling-based method for high-dimensional time-variant reliability analysis, Mechanical Systems and Signal Processing 126 (2019) 505–520.

[13] S. Chakraborty, S. Tesfamariam, Subset simulation based approach for space-time-dependent system reliability analysis of corroding pipelines, Structural Safety 90 (2021) 102073.

[14] W. Du, Y. Luo, Y. Wang, Time-variant reliability analysis using the parallel subset simulation, Reliability Engineering & System Safety 182 (2019) 250–257.

[15] X. Yuan, S. Liu, M. Faes, M. A. Valdebenito, M. Beer, An efficient importance sampling approach for reliability analysis of time-variant structures subject to time-dependent stochastic load, Mechanical Systems and Signal Processing 159 (2021) 107699.

[16] Y. Zhang, J. Xu, M. Beer, A single-loop time-variant reliability evaluation via a decoupling strategy and probability distribution reconstruction, Reliability Engineering & System Safety 232 (2023) 109031.

[17] Z. Xu, J. H. Saleh, Machine learning for reliability engineering and safety applications: Review of current status and future opportunities, Reliability Engineering & System Safety 211 (2021) 107530.

[18] M. Li, Z. Wang, Lstm-augmented deep networks for time-variant reliability assessment of dynamic systems, Reliability Engineering & System Safety 217 (2022) 108014.

[19] Z. Wang, P. Wang, A double-loop adaptive sampling approach for sensitivity-free dynamic reliability analysis, Reliability Engineering & System Safety 142 (2015) 346–356.

[20] I. Depina, T. M. H. Le, G. Fenton, G. Eiksund, Reliability analysis with metamodel line sampling, Structural Safety 60 (2016) 1–15.

[21] J. Wu, Z. Jiang, H. Song, L. Wan, F. Huang, Parallel efficient global optimization method: A novel approach for time-dependent reliability analysis and applications, Expert Systems with Applications 184 (2021) 115494.

[22] Z. Zhao, Z.-H. Lu, X.-Y. Zhang, Y.-G. Zhao, A nested single-loop kriging model coupled with subset simulation for time-dependent system reliability analysis, Reliability Engineering & System Safety 228 (2022) 108819.

[23] K. Zhang, N. Chen, P. Zeng, J. Liu, M. Beer, An efficient reliability analysis method for structures with hybrid time-dependent uncertainty, Reliability Engineering & System Safety 228 (2022) 108794.

[24] I. Papaioannou, D. Straub, Combination line sampling for structural reliability analysis, Structural Safety 88 (2021) 102025.

[25] X. Yuan, Y. Qian, J. Chen, M. G. Faes, M. A. Valdebenito, M. Beer, Global failure probability function estimation based on an adaptive strategy and combination algorithm, Reliability Engineering & System Safety 231 (2023) 108937.

[26] B. Sudret, A. Der Kiureghian, Stochastic finite element methods and reliability. A state-of-the-art-report, Technical Report November, Department of Civil & Environmental Engineering, University of California, Berkley, Institute of Structural Engineering, Mechanics and Materials, 2000.

[27] S. Huang, S. Quek, K. Phoon, Convergence study of the truncated karhunen–loève expansion for simulation of stochastic processes, International journal for numerical methods in engineering 52 (2001) 1029–1043.

[28] C.-C. Li, A. Der Kiureghian, Optimal discretization of random fields, Journal of Engineering Mechanics 119 (1993) 1136–1154.

[29] E. Vanmarcke, Random Fields: Analysis and Synthesis, MIT Press, Cambridge, 1983.

[30] K. K. Phoon, H. W. Huang, S. T. Quek, Simulation of strongly non-Gaussian processes using Karhunen-Loève expansion, Probabilistic Engineering Mechanics 20 (2005) 188–198.

[31] M. A. Valdebenito, H. A. Jensen, H. Hernández, L. Mehrez, Sensitivity estimation of failure probability applying line sampling, Reliability Engineering & System Safety 171 (2018) 99–111.

[32] H. Li, Z. Lü, X. Yuan, Nataf transformation based point estimate method, Chinese Science Bulletin 53 (2008) 2586–2592.

[33] T. W. Lee, B. M. Kwak, A reliability-based optimal design using advanced first order second moment method, Journal of Structural Mechanics 15 (1987) 523–542.

[34] M. A. Valdebenito, P. Wei, J. Song, M. Beer, M. Broggi, Failure probability estimation of a class of series systems by multidomain line sampling, Reliability Engineering & System Safety 213 (2021) 107673.

[35] J. Song, P. Wei, M. Valdebenito, M. Beer, Active learning line sampling for rare event analysis, Mechanical Systems and Signal Processing 147 (2021) 107113.

[36] R. Melchers, Importance sampling in structural systems, Structural safety 6 (1989) 3–10.